nature publishing group

Noninvasive monitoring of brain edema after hypoxia in newborn piglets

Shadi N. Malaeb[1], Meltem Izzetoglu[2], Jane McGowan[1] and Maria Delivoria-Papadopoulos[1]

BACKGROUND: Development of cerebral edema after brain injury carries a high risk for brain damage and death. The present study tests the ability of a noninvasive cerebral edema monitoring system that uses near-infrared spectroscopy (NIRS) with water as the chromophore of interest to detect brain edema following hypoxia.

METHODS: Ventilated piglets were exposed to hypoxia for 1 h, and then returned to normal oxygen levels for 4 h. An NIRS sensor was placed on the animal's head at baseline, and changes in light attenuation were converted to changes in H_2O. Cerebral water content and aquaporin-4 protein (AQP4) expression were measured.

RESULTS: The system detected changes in NIRS–derived water signal as early as 2 h after hypoxia, and provided fivefold signal amplification, representing a 10% increase in brain water content and a sixfold increase in AQP4, 4 h after hypoxia. Changes in water signal correlated well with changes in cerebral water content ($R = 0.74$) and AQP4 expression ($R = 0.97$) in the piglet brain.

CONCLUSION: The data show that NIRS can detect cerebral edema early in the injury process, thus providing an opportunity to initiate therapy at an earlier and more effective time-point after an insult than is available with current technology.

Brain injury is the leading cause of death and disability in the United States for infants, children, and young adults. Intrauterine lack of oxygen (hypoxia) and cerebral ischemia affect over 6,000 newborns every year in the United States, many of whom will not survive or will suffer severe lifelong brain damage resulting in cerebral palsy and other neurologic deficits (1). In older children, hypoxia-induced brain injury may occur as a complication of catastrophic events such as near drowning and cardiac arrest and of complex surgical procedures such as surgery to correct complex congenital heart disease (2). Traumatic brain injury, brain tumors, diabetic coma, and other acute neurologic events may also result in long-term neurologic deficits. The direct toll of brain injury is significant and the indirect costs to the child, his or her family, and the relevant social and education systems are many times greater, estimated to be well over one million US dollars per case (3).

Swelling of the brain, often referred to as cerebral edema, presents as increased brain volume resulting from excessive accumulation of either intracellular or extracellular fluid in the brain proper (4). Cerebral edema is classified into cytotoxic, vasogenic, osmotic, and hydrostatic mechanisms. Vasogenic edema results from breakdown of the blood–brain barrier and extravasation of fluid and proteins into the brain parenchyma, as well as from impaired cerebral autoregulation and fluid shifts from the systemic circulation into the brain. Cytotoxic edema results from abnormal water uptake by injured brain cells. Excessive fluid accumulation in the brain can result from a combination of cytotoxic and vasogenic edema. Cellular energy failure leads to failure of ATP-dependent sodium pumps such as the sodium potassium ATPase and results in intracellular sodium accumulation that is accompanied by influx of ions such as chloride and bicarbonate (5). Water shifts from the extracellular to the intracellular compartment down an osmotic gradient through dedicated water channels to maintain osmotic equilibrium. Aquaporins (AQPs) are integral membrane proteins that serve as molecular water channels that conduct water bidirectionally through the cell membrane down the osmotic gradient (6). AQP4 is uniquely expressed in astrocytes and is upregulated by insults to the brain (7,8). AQPs are dynamically regulated through different mechanisms such as subcellular distribution, orthogonal array formation, protein–protein interactions, channel gating, and phosphorylation (9,10). Phosphorylation of AQP4 is thought to be an important regulatory mechanism of its function, such that AQP4 becomes activated when phosphorylated at certain serine residues and is trafficked to the plasma membrane.

Studies have shown that cerebral edema following brain injury carries high risk for severe neurologic damage and death (11,12). Swelling of the brain results in increased intracranial pressure (ICP), which limits blood flow to the brain and can ultimately result in brain death if left untreated (13). Early identification of cerebral edema after brain injury

[1]Department of Pediatrics, Drexel University College of Medicine, St Christopher's Hospital for Children, Philadelphia, PA; [2]Department of Electrical and Computer Engineering, Villanova University, Villanova, PA. Correspondence: Shadi N. Malaeb (shadi.malaeb@drexel.edu)

Received 1 May 2017; accepted 25 September 2017; advance online publication 6 December 2017. doi:10.1038/pr.2017.264

Copyright © 2018 International Pediatric Research Foundation, Inc.

and initiation of interventions that can mitigate subsequent increases in ICP have become the mainstay of therapy for patients with severe head injury (14,15). Early and intensive management with vigorous surgical and medical therapy enable some patients who would have died otherwise to make a good recovery. The ability to monitor the progression of brain injury in real time is important to guide therapy (15).

Near-infrared spectroscopy (NIRS) is a portable noninvasive technology that detects changes in the way in which different molecules absorb and disperse emitted light at different wavelengths, which are visualized as colors. NIRS can be used to detect changes in oxygenated and deoxygenated hemoglobin associated with brain tissue hypoxia and estimate changes in cerebral blood volume and flow (16). The Optical Brain Imaging group at the Drexel University developed a novel NIRS–based flexible neuroimaging device that enables continuous real-time monitoring of changes in both blood and water content of the brain. In the present study, we used a newborn piglet model of hypoxic brain injury to investigate the ability of water-based NIRS technology to detect hypoxia-induced cerebral edema and assessed the correlation of the NIRS–derived water signal with increases in cerebral water content in the piglet brain after hypoxia.

METHODS

Animal Experiments

The animal protocol followed the guidelines of the National Research Council and was approved by the Institutional Animal Care and Use Committee at Drexel University. Newborn piglets (3–5 days old) were randomly assigned to either hypoxic or normoxic sham-control groups. A subgroup of normoxic piglets were subjected to whole-body hypothermia to study the effect of cooling on NIRS signal. A group of normal non-instrumented piglets was included to establish values for cerebral water content in healthy newborn piglets.

Induction of anesthesia. Anesthesia was induced with inhalation of 4% isoflurane. A peripheral intravenous catheter was inserted for administration of fluids and medications. Following intubation, the piglets were anesthetized, ventilated, and maintained on a balanced mix of oxygen and nitrous oxide gas. Intravenous fentanyl (50 μg/kg) was administered periodically to provide supplemental sedation and analgesia, and vecuronium (0.1 mg/kg) was administered intermittently as a paralytic agent to minimize risk of endotracheal tube dislodgement during the study period.

Induction of hypoxia and ischemia. Details of the hypoxia procedure were as described previously (17). The animals were allowed 1 h of baseline ventilation with normal blood gases and blood pressures, after which they were randomly assigned to either normoxia or hypoxia. Piglets in the normoxic groups were ventilated with 21% oxygen throughout the period of the study. In the hypoxic group, oxygen level decreased to ~7% within 5 min and maintained for an hour. The level of hypoxia was titrated to achieve target PaO_2 values of 20–24 mm Hg and a minimum 40% reduction in systolic blood pressure from baseline. $PaCO_2$ values were maintained between 35 and 45 mm Hg. Vital signs were recorded non-invasively every 15 min and included heart rate, blood pressure, and temperature. Continuous electrocardiogram and peripheral pulse-oximetry measurements were obtained and arterial blood gases were sampled to confirm hypoxia. Severe bradycardia or other arrhythmia were addressed with modest transient increases in inspired oxygen. Arterial blood gases were sampled at baseline and every 15 min during hypoxia exposure to confirm hypoxia and metabolic acidosis, and hourly thereafter. A superficial two-channel electroencephalogram was obtained at baseline and during the hypoxia period to ensure a significant decrease in amplitude during hypoxia. After exposure to hypoxia for 1 h, inspired oxygen was returned to normal levels for 4 h during which the animals were maintained at normal body temperature of 39 °C. Following this period, the animals were killed and the brains were harvested for biochemical analysis.

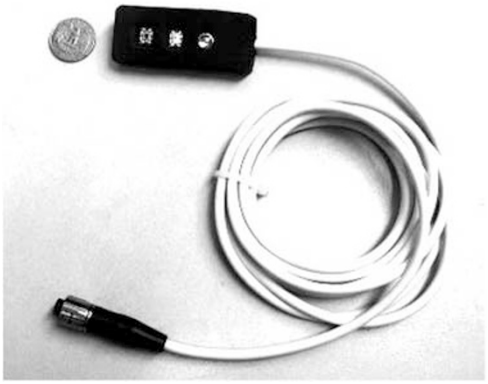

Figure 1. The near-infrared spectroscopy (NIRS) sensor built on a flexible circuit board having three light-emitting diodes and two photodetectors, one at 1.5 cm (near) and the other at 3 cm (far) distance away from the light sources. The sensor is covered with a flexible black foam for cushioning and insulation purposes.

NIRS monitoring and data analysis. The NIRS edema monitoring system (US Provisional Patent Application No. 62/152,377), developed by the Drexel University Optical Brain Imaging Group, consists of a custom-made sensor housing light sources and detectors, a data collection box, and a computer for data storage and presentation. The sensor was built on a flexible circuit board having three light-emitting diodes at 730, 850, and 940 nm wavelengths and two photodetectors one at 1.5 cm (near) and the other at 3 cm (far) distance away from the light-emitting diode-type light sources. The overall sensor was covered with a flexible black foam for cushioning and insulation purposes (**Figure 1**). There were two similar sensors built and can be operated by the data collection box which could collect data from them at 2 Hz sampling rate. One of the sensors was placed on the piglet's head on the frontoparietal region in between the ears using a double-sided medical grade tape to ensure good contact of the sensor with the skin and to eliminate the possibility of sensor movement during recording. Sensor placement region was trimmed before sensor placement to eliminate hair absorption and contact loss by the sensor. The other identical sensor was placed on one of the forelimbs of the animal to monitor simultaneous somatic signals during each recording. Initial recordings were obtained while the animals were awake and undisturbed to ensure functionality of the device. The probes were placed again after the animal had been anesthetized and ventilated. Baseline recordings of 30 min were obtained and zeroed as a reference point before the onset of hypoxia, and were recorded during hypoxia and until the end of the study period. Visual inspection confirmed that the signals contained minimal movement artifact. The raw intensity measurements were then filtered by a low-pass filter with cutoff frequency at 0.1 Hz to eliminate heart pulsation and respiration signals, as well as high-frequency noise. The low-pass filtered intensity measurements were then converted to changes in oxygenated hemoglobin (HbO_2), deoxygenated hemoglobin (Hb), and water content using the modified Beer–Lambert law (MBLL) using three wavelength measurements (16,18). We presumed the

Copyright © 2018 International Pediatric Research Foundation, Inc.

required values for MBLL conversion such as differential path length factors and extinction coefficients similar to the ones provided for infants (19,20). Changes in the chromophores (Hb, HbO_2, and water content) throughout the overall measurement period were obtained relative to a 10 s data segment within the first 30 min of the baseline region before the animal was exposed to hypoxia, and expressed as delta micromoles (Δμmol). In addition, the response of the NIRS signal to whole-body hypothermia was studied in normoxic piglets placed on a circulating water blanket and cooled to 33 ± 0.5 °C for 4 h after the baseline period and compared to normoxic normothermic controls.

Cerebral Water Content Measurements

Fresh samples obtained from the frontal–cerebral cortex were weighed before and after incubation for 72 h at 90 °C and cerebral water content was determined as wet weight minus dry weight divided by the dry weight of the tissue expressed in grams H_2O per gram tissue weight (g H_2O/g tissue). The brains were flash-frozen in liquid nitrogen for biochemical analyses.

Biochemical Assays

Protein content. Protein content was determined according to a modified version of the Pierce bicinchoninic acid protein assay (Pierce Biotechnology, Rockford, IL; catalog no. 23225). Serial dilutions of bovine serum albumin were prepared and stock bicinchoninic acid reagents including cupric sulfate were combined and incubated at room temperature for 2 h. Quantification of protein content occurred by measuring absorbance at a wavelength of 562 nm.

Aquaporin-4 Protein Expression

Frozen cerebral tissue was weighed and a 5% tissue homogenates were prepared using a dounce hand-held homogenizer in a modified RIPA buffer containing 10 mM Tris-HCl (pH 7.4), 1% Triton X-100, 1% sodium deoxycholate, 0.1% sodium dodecyl sulfate, 158 mM sodium chloride, 1mM EGTA, 0.1% Igepal CA 630, 2% aprotinin, and 2 mM sodium orthovanadate. The homogenate was centrifuged at 1,000*g* for 10 min, and the supernatant was centrifuged again at 40,000*g* for 1 h. The resulting pellet was resuspended again in the same buffer and centrifuged at 40,000*g* for 1 h for further purification. The final pellet, which contained the concentrated membrane fraction of the cerebral cortex, was resuspended in an equal volume of buffer and frozen at − 80 °C until the assay was performed. Equal amounts of membrane fraction protein (40 μg) from animals in each group were mounted on a gradient sodium dodecyl sulfate gel for western blot analysis. Membranes were blocked in 3% milk and probed with rabbit anti-AQP4 polycolonal primary antibodies (1:100; Abcam, Cambridge, MA; catalog no. ab46182) and goat anti-rabbit secondary antibodies (1:200; Abcam, Cambridge, MA; catalog no. 7090). The blots were developed using enhanced chemiluminescence (Pierce Biotechnology, Rockford, IL; catalog no. 32106). Actin was probed on the same blots to confirm homogenous loading and transfer of protein. Optical densities were determined using the Image J software (NIH, Bethesda, MD) and expressed as normalized ratios to the same normoxic control on each gel.

Statistical Analysis

All data are presented as mean ± s.d. or as 95% confidence intervals when applicable, and analyzed using one-way ANOVA for parametric data and post-hoc analysis using the Bonferroni correction. If conditions of normality and/or homogeneity of variance were not met, Kruskal-Wallis ANOVA on ranks test was applied. The Pearson's correlation coefficient was used to assess linear associations. We used the statistical software Sigma Plot version 13 (Systat Software, San Jose, CA). A *P*-value of <0.05 was considered statistically significant.

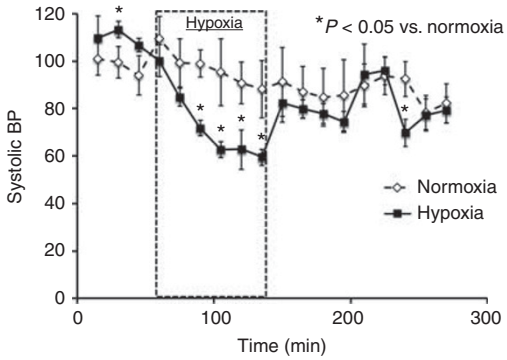

Figure 2. Blood pressure tracings from normoxic and hypoxic piglets. There was a significant reduction in systolic blood pressure during hypoxia exposure compared to controls.

RESULTS

Physiologic Parameters

Sixteen ventilated and anesthetized 3–5-day-old newborn piglets were assigned to either normoxia (Nx, $n=8$) or hypoxia (Hx, $n=8$) groups. Physiologic data from hypoxic piglets and from normoxic piglets during comparable periods of time were collected at normal body temperatures and compared between the two groups. Maximum reduction from baseline systolic blood pressure was 15 ± 3% in normoxic piglets and 55 ± 7% in hypoxic piglets (**Figure 2**; $P<0.05$). Lowest PaO_2 and pH were 91 ± 2 and 7.34 ± 1.28 mm Hg in normoxic piglets and 23 ± 6 and 7.08 ± 0.22 mm Hg in hypoxic piglets ($P<0.05$). The average amplitude of the electroencephalogram was 44.6 ± 7.0 μV at baseline ($n=7$), and decreased significantly within minutes of exposure to hypoxia and remained depressed throughout the hypoxia period. The amplitude of the electroencephalogram decreased by 86% at 30 min of hypoxia (6.2 ± 1.8 μV; $P<0.05$ vs. baseline) and reached 4.9 ± 2.4 μV at the end of hypoxia ($P<0.05$ vs. baseline). Body temperatures remained within normal range in the normothermic groups ($P=$NS), and within target range in the hypothermic group for the duration of the study (33.6 ± 0.6 °C; $n=5$; $P<0.01$ vs. normothermia).

Near-Infrared Spectroscopy

Deoxygenated hemoglobin (Hb) and oxygenated hemoglobin (HbO_2) signals were unchanged from baseline throughout the study period in all of the normoxic piglets. There was a predictable increase in Hb and decrease in HbO_2 during hypoxia in all of the hypoxic piglets, with a return to baseline levels after reoxygenation. The water signal tracing remained essentially flat during hypoxia, as well as over 4 h of recording in normoxic piglets (**Figure 3**, hatched line). In contrast, the NIRS cerebral water signal started to increase sharply soon after reoxygenation and continued to rise throughout the recording period in hypoxic animals (**Figure 3**, solid line). The rise in water signal tracing reached a statistically significant threshold after 2 h reoxygenation in hypoxic piglets, and after 5 h of recording in normoxic controls. The

Copyright © 2018 International Pediatric Research Foundation, Inc.

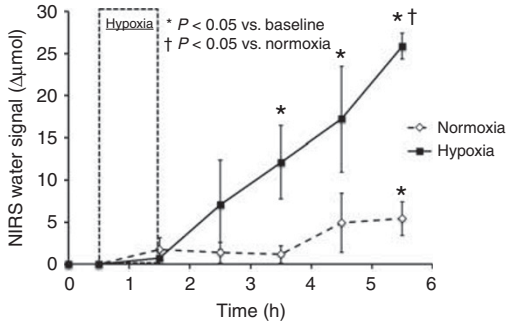

Figure 3. Changes in near-infrared spectroscopy (NIRS) water signal over time in normoxic and hypoxic normothermic piglets. The NIRS–derived water signal increased from baseline as early as 2 h after hypoxia, and was fivefolds higher in hypoxic piglets compared with normoxic piglets 4 h after hypoxia, with no overlap in the signal between the two groups.

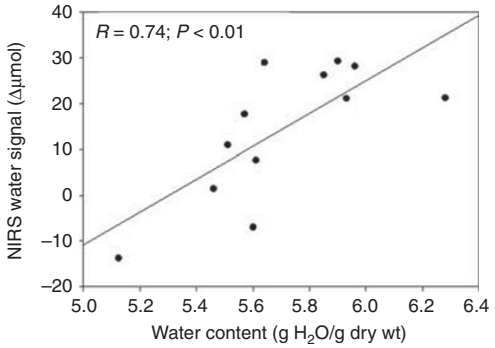

Figure 4. Correlation between changes in NIRS-derived water signal and changes cerebral water content in the cerebral cortex of newborn piglets. Of note, the water signal decreased from baseline in two of the piglets in the normoxia hypothermia group. Increases in cerebral water content correlated positively with the observed increases in the NIRS water signal.

NIRS–derived water signal increased by 5.4 ± 4.5 μmol from baseline in normoxic animals and by 25.8 ± 3.8 μmol in hypoxic animals 4 h after hypoxia when the animals were maintained at normal body temperatures following hypoxia ($P < 0.05$; **Figure 3**). Notably, there was no overlap in the NIRS–derived water signal between the two groups at the 4-hour end point of the study (95% confidence interval (CI): 21.9, 29.8 in Hx vs. −0.1, 11.0 in Nx). The NIRS–derived water signal did not change significantly from baseline in normoxic animals after 4 h of hypothermia (0.2 ± 5.6 μMol; $n = 5$; P = NS vs. normothermia). The edema monitoring system provided early detection of cerebral edema as early as 2 h after the insult, and over sixfolddifference in the water signal between normoxic and hypoxic piglets 4 h after hypoxia ($P < 0.05$).

Cerebral Water Content

Cerebral water content in noninstrumented healthy 3–5-day-old piglets was 5.39 ± 0.10 g H_2O/g tissue ($n = 3$). Cerebral water content was 5.45 ± 0.28 g H_2O/g tissue in normoxic normothermic piglets and 5.55 ± 0.32 g H_2O/g tissue in normoxic hypothermic piglets, both comparable to that seen in noninstrumented healthy piglets (P = NS). In contrast, cerebral water content increased to 5.89 ± 0.19 g H_2O/g tissue in hypoxic piglets 4 h after hypoxia ($P < 0.05$ vs. Nx). Changes in NIRS–derived water signal correlated positively with changes in cerebral water content in the piglet brain (**Figure 4**; $n = 12$; $R = 0.74$; $P < 0.01$).

AQP4 Protein Expression

Western blot analysis of AQP4 protein expression in equal loads of the membrane fraction of cerebral cortical extracts showed a sixfold increase in AQP4 expression in hypoxic piglets 4 h after hypoxia compared with normoxic controls (**Figure 5**; $P < 0.01$). Increased AQP4 protein expression correlated positively with increases in NIRS–derived water signal in the piglet brain (**Figure 6**; $n = 6$; $R = 0.97$; $P < 0.01$).

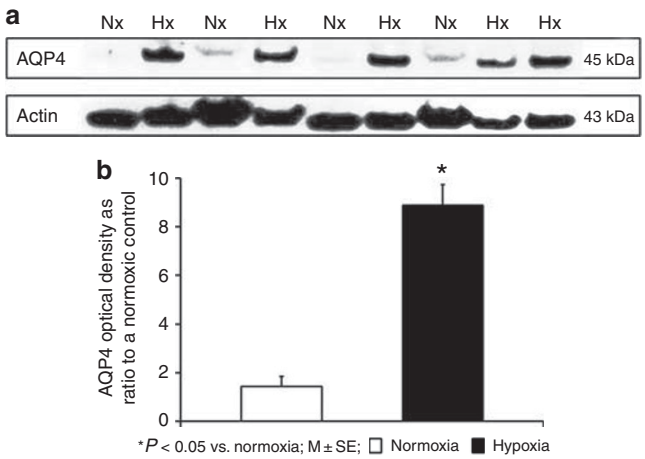

Figure 5. Aquaporin-4 (AQP4) protein expression in the membrane fraction of the cerebral cortex in normoxic (Nx) and hypoxic (Hx) normothermic piglets. (**a**) A representative western blot of AQP4 protein in normoxic and hypoxic piglets. (**b**) The optical densities of AQP4 bands as the ratio of AQP4 band normalized to samples obtained from the same normoxic brain and represented as means and standard errors of normoxic and hypoxic groups. AQP4 expression increased significantly by 4 h after hypoxia.

DISCUSSION

The data show significant increases in AQP4 water channel protein expression in the cerebral cortex of newborn piglets following exposure to hypoxia, and this increased expression correlated with small but significant increases in brain water content after hypoxia. The NIRS–based edema monitoring system detected changes in the NIRS–derived water signal as early as 2 h after hypoxia, and provided a sensitive, accurate, fivefold signal amplification that allowed detection of a relatively subtle 10% increase in brain water content 4 h after onset of hypoxia. The NIRS signal intensity did not change from baseline during whole-body hypothermia.

Copyright © 2018 International Pediatric Research Foundation, Inc.

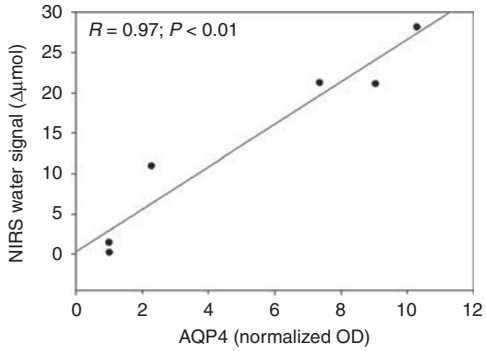

Figure 6. Correlation between changes in NIRS-derived water signal and aquaporin protein expression in the cerebral cortex of normothermic newborn piglets. Increases in aquaporin-4 water channel protein expression correlated positively with the observed increases in the NIRS water signal.

We used a well-characterized large animal model of hypoxia to study the effect of hypoxia on cerebral water regulation in newborn piglets (17,21,22). Physiologic data from the animals confirm that the applied hypoxic insult resulted in cerebral tissue hypoxia and induction of the apoptotic cascade. Delivoria-Papadopoulos and co-workers (23–25) have previously documented significant increases in kinase and phosphatase enzyme activities in the cerebral cortex after acute hypoxia in a similar newborn piglet model. We propose that cerebral energy failure secondary to hypoxia alters kinase and phosphatase balance in the cell and affects the phosphorylation state of proteins such as AQP4, which facilitates its recruitment to the plasma membrane. Increased water channel expression results in cellular swelling and disruption of astrocytic functions such as neurotrophic support and reuptake of excitotoxic neurotransmitters, which can subsequently contribute to neuronal cell death. Intravenous fluid administration and general anesthesia may have partially contributed to increases in cerebral water content from baseline seen in hypoxic piglets and in normoxic controls, when compared with healthy noninstrumented piglets.

Cerebral edema has been shown to occur as early as 1 h after hypoxia in animal models. Lingwood *et al.* (26) studied the development of cerebral edema in hypoxic piglets exposed to 4–6% oxygen and measured the increase in cerebral bioimpedance measured both noninvasively using gel electrodes attached to the scalp and invasively using subdural electrodes alongside a catheter placed for continuous ICP monitoring. They demonstrated significant increases in cerebral water content and ICP as early as 1 hour after the insult in hypoxic piglets. Noninvasive monitoring showed an increase in cerebral bioimpedence in piglets exposed to severe, but not mild hypoxia. Thiagarajah *et al.* (27) used noninvasive NIRS technology to detect brain swelling in adult mice using a fixed mount beam apparatus. They showed that light scattering at 850 nm wavelength increased within minutes of acute water intoxication and correlated with increases in brain water as measured by wet-to-dry weight ratios, and with increases in ICP. Interestingly, changes in optical signal occurred significantly earlier than changes in ICP in these animals. Qiao *et al.* (28) reported increases in cerebral water content as early as 1 h after exposure to hypoxia and ischemia in 1-week-old rats exposed to hypoxia and unilateral carotid artery ligation, as measured by changes in T1 signals on magnetic resonance imaging and validated by wet and dry weight difference of cerebral tissue. However, magnetic resonance imaging failed to demonstrate cerebral edema shortly after hypoxic ischemic injury in other models. Apparent diffusion coefficients followed over 48 h in piglets exposed to transient hypoxia–ischemia showed statistically significant increases in water signals to be first visible ~ 12 h after the end of the hypoxic–ischemic insult (29).

Currently, cerebral edema is most accurately identified clinically using either computed tomography scan or diffusion-weighted magnetic resonance imaging showing increased cerebral water content (30,31). However, critically ill patients often cannot tolerate transport to undergo imaging studies. Moreover, current ICP monitoring in critically ill patients requires invasive neurosurgical procedures (15). Invasive ICP monitoring is not without significant risks to the patient including but not limited to life-threatening infection, head bleeds, intracranial bleeding, pain, and anesthesia risks. In addition, these procedures require a high level of expertise that is generally only available in a few advanced medical care centers, thus requiring transfer of the patient to another facility. Head ultrasonography is one portable noninvasive technology used to detect cerebral edema after brain injury (32). However, ultrasound has more limited tissue characterization capabilities than computed tomography or magnetic resonance imaging, and the magnitude of difference seen on head ultrasound following hypoxic brain injury in the first 24–48 h is often mild (33). Head ultrasonography obtained at 24–48 h of life showed only a small 16.4% difference in the white to grey matter echogenicity ratios at the level of the cingulate gyrus between term human infants who suffered from perinatal hypoxic–ischemic encephalopathy and matched controls. Moreover, there was a significant degree of overlap in the ranges of the signal between the two groups (33). Transcranial Doppler sonography is another technology that applies measurements of cerebral blood flow velocities to estimate changes in ICP after brain injury; however, it is limited by spatial and interobserver variability and is technically demanding, which confines its widespread applicability (34,35). Therefore, there remains a need for a noninvasive portable and sensitive technique that is able to detect early manifestations of cerebral edema following brain injury and present a safe and accurate alternative that could be used to guide subsequent medical and surgical management in a timely manner and improve outcomes.

Our study is the first to demonstrate the ability of a noninvasive cerebral edema monitoring system that utilizes NIRS technology with water as the chromophore of interest to

Copyright © 2018 International Pediatric Research Foundation, Inc.

detect safely and reliably early changes of cerebral edema in a clinically relevant model of hypoxic brain injury in newborn piglets. The system provided early detection of cerebral edema signal as early as 2 h post hypoxia, and a fivefold discrimination power between normoxic and hypoxic piglets with no overlap in the water signal between the two groups.

There are several limitations to our study. First, a limitation of the present study is that it is not possible to separate the contribution of individual layers along the path length such as skin, scalp, and subarachnoid space to the total signal. To minimize this limitation, we used a unique deep tissue sensor with a 3 cm source-detector separation derived from our previous post-mortem studies of sagittal sections of the newborn piglet head to ensure that the majority of the change in the optical signal originated from changes in water content in the cerebral cortex proper. Pilot studies in our model showed that the probe can be reapplied at same position without changes in the NIRS signal. Another limitation relates to the differences between the pig and human skull could affect the measurements of water changes in human infants. The present study was not intended to explore the absolute values required for modified Beer–Lambert law conversion in piglets; rather, it focuses on behavior of the NIRS signal over time, and uses the same presumed values in all piglets and compares them among each other and over time. It was beyond the scope of the present study to obtain further neuroimaging or to perform invasive ICP measures after hypoxia in these piglets. Despite limitations, our noninvasive cerebral edema monitoring system was able to detect a significant change in cerebral water that correlated well with well-defined markers of cerebral edema such as cerebral water content and water channel protein expression.

We conclude that cerebral edema develops shortly after hypoxia in the newborn. The data show that water-based NIRS technology can reliably detect manifestations of cerebral edema after hypoxia in newborn piglets. Our findings suggest that NIRS–based edema monitoring can provide sensitive technology to detect cerebral edema early in a critical time window between the occurrence of a hypoxic event and initiation of therapeutic intervention. This potential opens a window of opportunity to initiate neuroprotective interventions at an earlier and more effective point in time after the hypoxic insult than is available with current technology.

ACKNOWLEDGMENTS

We thank Baruch Ben Dor, John Grothusen, Juan Du, and Jessica Button for their technical assistance. This project was funded, in part, under a grant with the Pennsylvania Department of Health SAP Number: 4100068711, and by the Coulter-Drexel Translational Research Partnership Program under grant number: 282812-3850.

STATEMENT OF FINANCIAL SUPPORT

This project was funded, in part, under a grant with the Pennsylvania Department of Health SAP Number: 4100068711, and by the Coulter-Drexel Translational Research Partnership Program under grant number: 282812-3850.

Disclosure: The authors declare no conflict of interest.

REFERENCES

1. Kurinczuk JJ, White-Koning M, Badawi N. Epidemiology of neonatal encephalopathy and hypoxic–ischaemic encephalopathy. Early Hum Dev 2010;86:329–38.
2. Hinduja A, Gupta H, Yang JD, et al. Hypoxic ischemic brain injury following in hospital cardiac arrest—lessons from autopsy. J Forensic Leg Med 2014;23:84–6.
3. Eunson P. The long-term health, social, and financial burden of hypoxic–ischaemic encephalopathy. Dev Med Child Neurol 2015;57(Suppl 3): 48–50.
4. Nag S, Manias JL, Stewart DJ. Pathology and new players in the pathogenesis of brain edema. Acta Neuropathol 2009;118:197–217.
5. Pasantes-Morales H, Vazquez-Juarez E. Transporters and channels in cytotoxic astrocyte swelling. Neurochem Res 2012;37:2379–87.
6. Benga G. Water channel proteins: from their discovery in 1985 in Cluj-Napoca, Romania, to the 2003 Nobel Prize in Chemistry. Cell Mol Biol (Noisy-le-grand) 2006;52:10–9.
7. Amiry-Moghaddam M, Frydenlund DS, Ottersen OP. Anchoring of aquaporin-4 in brain: molecular mechanisms and implications for the physiology and pathophysiology of water transport. Neuroscience 2004;129:999–1010.
8. Potokar M, Jorgacevski J, Zorec R. Astrocyte aquaporin dynamics in health and disease. Int J Mol Sci 2016: 17.
9. Assentoft M, Larsen BR, MacAulay N. Regulation and function of AQP4 in the central nervous system. Neurochem Res 2015;40:2615–27.
10. Yukutake Y, Yasui M. Regulation of water permeability through aquaporin-4. Neuroscience 2010;168:885–91.
11. Feickert HJ, Drommer S, Heyer R. Severe head injury in children: impact of risk factors on outcome. J Trauma 1999;47:33–8.
12. Lupton BA, Hill A, Roland EH, et al. Brain swelling in the asphyxiated term newborn: pathogenesis and outcome. Pediatrics 1988;82:139–46.
13. Nakagawa TA, Ashwal S, Mathur M, et al. Clinical report—Guidelines for the determination of brain death in infants and children: an update of the 1987 task force recommendations. Pediatrics 2011;128e720-40.
14. Becker DP, Miller JD, Ward JD, et al. The outcome from severe head injury with early diagnosis and intensive management. J Neurosurg 1977;47:491–502.
15. Bullock MR, Povlishock JT. Guidelines for the management of severe traumatic brain injury. Editor's Commentary. J Neurotrauma 2007;24 (Suppl 1): 2 p preceding S1.
16. Cope M, Delpy DT. System for long-term measurement of cerebral blood and tissue oxygenation on newborn infants by near infra-red transillumination. Med Biol Eng Comput 1988;26:289–94.
17. Ashraf QM, Zubrow AB, Mishra OP, et al. Nitration of Bax and Bcl-2 proteins during hypoxia in cerebral cortex of newborn piglets and the effect of nitric oxide synthase inhibition. Biol Neonate 2002;81:65–72.
18. Izzetoglu M, Bunce SC, Izzetoglu K, et al. Functional brain imaging using near-infrared technology. IEEE Eng Med Biol Mag 2007;26:38–46.
19. Bozkurt A, Rosen A, Rosen H, et al. A portable near infrared spectroscopy system for bedside monitoring of newborn brain. Biomed Eng Online 2005;4:29.
20. Wyatt JS, Cope M, Delpy DT, et al. Measurement of optical path length for cerebral near-infrared spectroscopy in newborn infants. Dev Neurosci 1990;12:140–4.
21. DiGiacomo JE, Pane CR, Gwiazdowski S, et al. Effect of graded hypoxia on brain cell membrane injury in newborn piglets. Biol Neonate 1992;61:25–32.
22. Thoresen M, Haaland K, Loberg EM, et al. A piglet survival model of posthypoxic encephalopathy. Pediatr Res 1996;40:738–48.
23. Ashraf QM, Haider SH, Katsetos CD, et al. Nitric oxide-mediated alterations of protein tyrosine phosphatase activity and expression during hypoxia in the cerebral cortex of newborn piglets. Neurosci Lett 2004;362:108–12.
24. Mami AG, Ballesteros JR, Fritz KI, et al. Effects of magnesium sulfate administration during hypoxia on CaM kinase IV and protein tyrosine kinase activities in the cerebral cortex of newborn piglets. Neurochem Res 2006;31:57–62.

Copyright © 2018 International Pediatric Research Foundation, Inc.

25. Mishra OP, Delivoria-Papadopoulos M. Effect of hypoxia on protein tyrosine kinase activity in cortical membranes of newborn piglets—the role of nitric oxide. Neurosci Lett 2004;372:114–8.
26. Lingwood BE, Dunster KR, Colditz PB, et al. Noninvasive measurement of cerebral bioimpedance for detection of cerebral edema in the neonatal piglet. Brain Res 2002;945:97–105.
27. Thiagarajah JR, Papadopoulos MC, Verkman AS. Noninvasive early detection of brain edema in mice by near-infrared light scattering. J Neurosci Res 2005;80:293–9.
28. Qiao M, Meng S, Scobie K, et al. Magnetic resonance imaging of differential gray versus white matter injury following a mild or moderate hypoxic-ischemic insult in neonatal rats. Neurosci Lett 2004;368:332–6.
29. Thornton JS, Ordidge RJ, Penrice J, et al. Temporal and anatomical variations of brain water apparent diffusion coefficient in perinatal cerebral hypoxic–ischemic injury: relationships to cerebral energy metabolism. Magn Reson Med 1998;39:920–7.
30. Kim JJ, Gean AD. Imaging for the diagnosis and management of traumatic brain injury. Neurotherapeutics 2011;8:39–53.
31. Lee B, Newberg A. Neuroimaging in traumatic brain imaging. NeuroRx 2005;2:372–83.
32. Kudreviciene A, Basevicius A, Lukosevicius S, et al. The value of ultrasonography and Doppler sonography in prognosticating long-term outcomes among full-term newborns with perinatal asphyxia. Medicina (Kaunas) 2014;50:100–10.
33. Pinto PS, Tekes A, Singhi S, et al. White-gray matter echogenicity ratio and resistive index: sonographic bedside markers of cerebral hypoxic-ischemic injury/edema? J Perinatol 2012;32:448–53.
34. Hanlo PW, Gooskens RH, Nijhuis IJ, et al. Value of transcranial Doppler indices in predicting raised ICP in infantile hydrocephalus. A study with review of the literature. Childs Nerv Syst 1995;11:595–603.
35. Tzeng YC, Ainslie PN, Cooke WH, et al. Assessment of cerebral autoregulation: the quandary of quantification. Am J Physiol Heart Circ Physiol 2012;303:H658–71.

Copyright © 2018 International Pediatric Research Foundation, Inc.